Journal of Machine Learning and Information Security
https://www.sciltp.com/journals/jmlis

Article

Fixed-Time Consensus of Nonlinear Multi-Agent Systems with Uncertain Disturbances via Saturation Constraint Impulsive Control

Shasha Yang [1,2,*], Lili Zhang [3], Jie Wang [3], Xinxin Jiang [3] and Lianghao Ji [1,2]

[1] Chongqing Key Laboratory of Image Cognition, Chongqing University of Posts and Telecommunications, Chongqing 400065, China
[2] Chongqing Key Laboratory of Computational agents, Chongqing University of Posts and Telecommunications, Chongqing 400065, China
[3] School of Communication and Information Engineering, Chongqing University of Posts and Telecommunications, Chongqing 400065, China
* Correspondence: yangss@cqupt.edu.cn

How To Cite: Yang, S.; Zhang, L.; Wang, J.; et al. Fixed-Time Consensus of Nonlinear Multi-Agent Systems with Uncertain Disturbances via Saturation Constraint Impulsive Control. *Journal of Machine Learning and Information Security* **2026**, *2*(1), 7. https://doi.org/10.53941/jmlis.2026.100007

Received: 16 December 2025
Revised: 18 March 2026
Accepted: 23 March 2026
Published: 27 March 2026

Abstract: This study investigates the consistency problem of nonlinear multi-agent systems (NMASs) when subjected to state-constrained impulsive control and uncertainty disturbances. To overcome the challenges posed by idealized simulation environments and the difficulty of obtaining consensus convergence-time initial conditions, we propose a control protocol that combines a state-constrained impulsive control strategy with a fixed-time (FT) consensus control strategy. The system dynamics model also accounts for uncertainty disturbances and semi-Markov switching topologies (SMSTs) to better approximate real-world systems. We introduce relevant theorems and assumptions necessary for theoretical analysis and simplify the theoretical analysis using Lyapunov stability theory, saturation function theory, and comparative system methods. Simulation results illustrate that the proposed system model can achieve consistency even in the presence of uncertainty. These findings provide empirical evidence to validate the effectiveness of the theoretical results.

Keywords: state-constrained impulsive control; fixed-time consensus; semi-markovian switching topologies; nonlinear multi-agent systems

1. Introduction

The distributed cooperative control of Nonlinear Multi-Agent Systems (NMASs) has garnered widespread academic interest over the past decade due to its critical role in multi-robot networking and smart grids. These systems are increasingly applied in various domains such as robot formations, sensor networks, and smart grids [1–4].

Yet, the real challenge lies in the execution. If we truly want to guarantee cooperative behavior across these systems, we inevitably have to tackle a fundamental prerequisite: ensuring that the individual agents within them are entirely on the same page. Naturally, robust control strategies are the key to unlocking such consistency. Currently, the field is driven by a diverse set of innovative approaches, including the widely discussed event-triggered and impulsive control methodologies. For example, Wang et al. [5] introduced an innovative control strategy amalgamating hierarchical control and event-triggered policies to address challenges in uncertain NMASs with unknown control directions. Similarly, other investigations [6] have utilized event-triggered strategies to resolve consistency issues in NMASs featuring nonlinear dynamics and uncertain disturbances. But here is the catch: we want peak performance, yet we cannot afford infinite communication. To strike this delicate balance, recent breakthroughs have turned to data-based event-triggered mechanisms. These have proven remarkably effective in navigating the treacherous waters of cooperative optimal output regulation, even within the most dauntingly complex nonlinear multi-agent systems [7]. Nonetheless, these methodologies typically employ continuous control techniques, thereby engendering communication resource inefficiencies.

Realizing that continuous control is often an expensive overkill, recent studies have nudged the field toward impulsive control [8–10]. Yet, real-world noise often triggers erratic impulses that threaten to destabilize the system. To counter this, saturation-aware impulsive strategies have emerged as a robust workaround for restoring control performance [11–14].

Beyond mere consistency, the quest for faster convergence has taken center stage. We've seen some ingenious attempts to push this envelope; for instance, [15] wedded neural networks with finite-time theorems to sharpen system response. In a similar vein, the work in [16] leveraged Integral Sliding Mode Control to tackle heterogeneity. However, a stubborn bottleneck remains: many of these solutions are still shackled to initial states and tuning parameters. In the unpredictable world of real-world deployment, not knowing the exact "finish time" beforehand remains a significant dealbreaker.

To break this deadlock, the spotlight has shifted toward Fixed-Time (FT) control methodologies—a true game-changer in the field. The real allure of FT control, as championed by [17], lies in its ability to guarantee convergence within a predictable window, effectively liberating the system from the unpredictability of its initial states. This paradigm shift has paved the way for more sophisticated designs, from the intricate timing observers and tracking controllers in [18] to the clever integration of event-triggered logic [6] that tackles FT consistency head-on.

It is one thing to achieve consistency on a blackboard, but quite another to maintain it in the wild. Lately, the field has moved toward a more grounded consensus: the real hurdles for NMASs aren't just mathematical, but environmental—specifically the unpredictable noise and disturbances that define real-world deployments [19,20]. These disturbances may perturb system states, thereby affecting the efficacy of control strategies. Nature is a challenge, but malice is a different beast entirely. Beyond unpredictable environmental noise, MASs must now contend with deliberate disruptions like Denial-of-Service (DoS) attacks. To bridge this security gap, some compelling recent work [21] has married neural networks with integral reinforcement learning. This synergy doesn't just "solve" cooperative output regulation in messy nonlinear systems; it builds a resilient shield that allows optimal control to finally hold its own in a truly hostile digital landscape. Concurrently, the network states of NMASs are influenced by communication topology, and fixed communication topology may lead to communication interruptions or the emergence of new information transmission paths. In addressing these challenges, researchers have begun focusing on NMASs influenced by Semi-Markov Switching Topologies (SMSTs) [14,22–25], introducing heightened complexity and randomness.

Drawing inspiration from the foundation laid by [14], we've opted for a convex combination approach. By remapping input-saturated impulsive signals into the more manageable geometry of convex polytopes, we effectively strip away the unnecessary computational baggage that often clogs these types of optimizations. By pivoting to FT control, we've effectively broken the shackles of initial state dependence that often haunt finite-time methods. This work isn't just about speed; it is about providing rock-solid stability guarantees within a predictable window, even under the added pressure of state constraints. To make our findings truly relevant, we've also introduced uncertain disturbances and utilized SMSTs to capture the raw, stochastic pulse of natural systems.

Furthermore, this thesis makes several significant contributions:

1. Traditional impulsive strategies often operate blindly, but introducing state constraints fundamentally changes the game. This framework introduces an "on-demand" agility: it scales the control intensity with the actual urgency of the system, naturally preventing resource overkill. Because the control action is intimately tied to the fluctuating states of individual agents, the network gains a profound resilience. It absorbs environmental volatility seamlessly while keeping a tight, efficient grip on overall consistency.
2. Stepping away from the restrictive initial-state dependencies of finite-time methods, the FT protocol champions a more robust, deployment-ready architecture. Its defining feature is its fluidity: the network topology actively morphs based on the relative distances between agents. This spatial agility ensures that the system doesn't just endure complex environments, but actively optimizes its connections to maintain seamless, reliable consensus.
3. Acknowledging that environmental noise can derail traditional fixed networks, this paper advocates for a resilient architecture rooted in switching topologies. The integration of SMSTs allows us to model the inherent randomness of practical communication links with high fidelity. By grounding the control logic in this stochastic framework, the proposed strategy effectively anchors system consistency, providing a reliable safety net that maintains peak performance amidst the chaos of external disturbances.

The paper is organized into five sections: Section 2 introduces relevant lemmas and definitions, providing a brief overview of the problem model involving graph theory, Semi-Markovian processes, state constraints, and more. Section 3 presents the proof procedure for the convergence of NMASs within a fixed time and derives expressions for specific time intervals. Section 4 conducts numerical simulations to demonstrate feasibility, and Section 5 concludes the paper.

Table 1 lists the symbols used in this document.

Table 1. Table of notations.

Symbol	Definition
R^m	m-dimensional Euclidean apace
N^+	Set of positive integers
P	Probability measure
E	Mathematical expectation
I_M	M-dimensional identity matrix
C^T	the transpose of matrix C
$diag\{\cdot\}$	Block-diagonal matrix
$\|*\|$	Euclidian norm
$\|*\|$	Absolute value
$\lambda_2(L)$	The second smallest eigenvalue of matrix L
$E(\cdot)$	Mathematical expectation

2. Preliminaries

2.1. Graph Theory

A communication topology that describes the network connectivity among N agents in NMASs is represented by $G^{\sigma(t)} = \left\{\vartheta, \mathcal{E}^{\sigma(t)}, \Lambda^{\sigma(t)}\right\}$, where $\sigma(t)$ is denoted as the switching signal of the system topology, and a known set of topologies $G^{\sigma(t)} = \left\{G_1^{\sigma(t)}, G_2^{\sigma(t)}, \ldots, G_s^{\sigma(t)}\right\}$, where $s \geq 1$. The node set $\vartheta = \{\upsilon_1, \upsilon_2, \ldots, \upsilon_n\}$ comprises individual agents, and $\mathcal{E}^{\sigma(t)} \subseteq \upsilon_i \times \upsilon_j$ defines the set of edges in the topology, where each edge represents a connection between two nodes in the agent set. The adjacency matrix $\Lambda^{\sigma(t)} = \left(a_{ij}^{\sigma(t)}\right)_{N\times N}$ describes the connectivity of the graph. If agent j is a neighbor of agent i, then $a_{ij}^{\sigma(t)} > 0$. Otherwise, $a_{ij}^{\sigma(t)} = 0$. The in-degree matrix is defined as $D^{\sigma(t)} = diag\left\{d_1^{\sigma(t)}, d_2^{\sigma(t)}, \ldots, d_N^{\sigma(t)}\right\}$, $d_i^{\sigma(t)}$ represents the in-degree of agent i at time t, and $deg\left(d_i^{\sigma(t)}\right) = \sum_{i=1}^{N} a_{ij}^{\sigma(t)}$. The Laplacian matrix $L^{\sigma(t)}$ is then obtained by subtracting the adjacency matrix $\Lambda^{\sigma(t)}$ from the in-degree matrix $D^{\sigma(t)}$, $L^{\sigma(t)} = D^{\sigma(t)} - \Lambda^{\sigma(t)}$.

2.2. Semi-Markovian Process

Lemma 1. *[9, 26]: The switching signal $\{\sigma(t), t \geq 0\}$ is said to be semi-Markovian switching, if let $\sigma(t) = \sigma(t_k) = \sigma(k)$ for $t \in [t_k, t_{k+1})$, $k \geq 0$, for $\mu \in S = \{1, 2, \cdots s\}$,*

$$\lim_{t\to\infty} \frac{T_\mu(t)}{t} = \pi_\mu, \ a.s., \ \forall \mu \in S$$
$$\lim_{t\to\infty} \frac{N_\mu(t)}{t} = \frac{\pi_\mu}{m_\mu}, \ a.s., \ \forall \mu \in S$$

Here, $T_\mu(t)$ and $N_\mu(t)$ denote the total time of stay and the total number of activations of the μ-th topology on $[0, t]$, m_μ represents the expected dwell time on the μ-th topology, $\pi_\mu = \frac{\bar{\pi}_\mu m_\mu}{\sum_{\upsilon\in S} \bar{\pi}_\upsilon m_\upsilon}$ represents the stationary distribution of $\sigma(t)$, and $\pi = (\pi_1, \pi_2, \cdots, \pi_s)$ denotes the overall stationary distribution.

Definition 1. *[9, 26]: Let $\{\sigma_k, k \in N\}$ represent a semi-Markov chain. The probability $\pi_{\mu\upsilon}$ denotes the probability of transitioning from the υ-th topology to the μ-th topology at time t_{k+1}, given that the current topology is $\sigma(t_k) = \upsilon$. Therefore, the transition probability matrix for the entire semi-Markov process is defined as:*

$$\Pi = [\pi_{\mu\upsilon}]_{s\times s}, \mu, \upsilon \in S = \{1, 2, \cdots s\}$$

For the μ-th topology, the dwell time is defined as τ_μ, and $\tau_\mu(k)$ represents the dwell time for the k-th impulsive event.

Definition 2. *The impulsive sequence is a part of $B(\tau_{min}, \tau_{max})$, where $B(\tau_{min}, \tau_{max})$ is defined as*

$$B(\tau_{min}, \tau_{max}) = \{\tau_{min} < \Delta T < \tau_{max}\}$$

Here, τ_{min} and τ_{max} are positive constants, and $\tau_{min} < \tau_{max}$. The impulsive interval is denoted as $\Delta T = t_k - t_{k-1}$,$0 < t_0 < \cdots < t_k$. Furthermore, $\lim_{t\to\infty} t_k = \infty$. Let $N(s,t)$ denote the number of impulsive events that occur in the interval (s,t). For an impulsive sequence belonging to $B(\tau_{min}, \tau_{max})$, the following condition holds:

$$\frac{t-s}{\tau_{max}} - 1 \leq N(s,t) \leq \frac{t-s}{\tau_{min}}$$

Definition 3. *[9] Consider the case of a semi-Markovian switched topology $G^{\sigma(t)}$ and an impulsive sequence $\{t_k, k \in N^+\}$, where the impulsive intervals satisfy $\tau_{\min} \leq \Delta T \leq \tau_{\max}$. If one defines $\widetilde{N}(s,t)$ as the number of impulsive controls that occur within the interval $[s,t]$, then an alternative expression for this can be given as follows:*

$$\frac{(t-s)}{\tau_{\max}} - \sum_{\mu\in S} \frac{\pi_\mu}{m_\mu} \leq \widetilde{N}(s,t) \leq \frac{(t-s)}{\tau_{\min}}$$

2.3. Saturation Function

In practical industrial systems, it is often necessary to impose constraints on the states of individual agents to ensure that the system operates within specific conditions. One way to enforce these constraints is by using a saturation function.

The saturation function is denoted as $sat(p)$ and is defined to limit the value of p within a specified range and can be understood in the following way:

$$sat(p) = \begin{cases} a & p > a \\ p & -a \leq p \leq a \\ -a & p < -a \end{cases} \tag{1}$$

Remark 1. *In the given expression, the upper and lower bounds of the saturation function are described as fixed values of $a = 1$. However, it is important to note that in practical industrial systems, the range of saturation limits can be dynamically adjusted based on specific requirements, allowing for a more flexible definition of variable constraints.*

2.4. Problem Formulation

To better introduce the theory in this paper, the dynamics model is set up as NMASs consisting of N agents, where the equations describe the dynamics of each agent:

$$\dot{p}_i(t) = u_i(t) + f(p_i(t), t) + d(p_i(t), t) \tag{2}$$

Here, $i = 1, 2, \ldots, N$, $p_i(t) \in R^n$ represents the state of the i-th agent, $f(p_i(t), t)$ is a continuous and differentiable nonlinear function, $d(p_i(t), t)$ represents an uncertain disturbance, and $u_i(t)$ denotes the control protocol for NMASs, which will be set in Section 3. The expression for setting up an impulsive differential system with a fixed impulsive interval is as follows:

$$\begin{cases} \dot{p}(t) = l(t, p(t)), \ t \neq t_k, \ k \in N \\ \Delta p(t) = p\left(t_k^+\right) - p\left(t_k^-\right) = S_k(p), \ t = t_k \end{cases} \tag{3}$$

where $l(t, p(t))$ denotes a function on $p(t)$, $S_k(p)$ is the impulsive-hopping value, and $\{t_k\}$ is a impulsive time series satisfying $0 = t_0 < t_1 < \cdots < t_k \cdots, k \to \infty$.

Definition 4. *Set the existence of a function $V(p,t)$ that satisfies the following conditions:*

$$\begin{cases} V(p,t) \leq g(V(p,t),t), & t \neq t_k \\ V(p + S_k(p), t) \leq \psi_k(V(p,t)), & t = t_k \end{cases}$$

where $g(V(p,t),t)$ represents a continuous expression in terms of $V(p,t)$, and $\psi_k(\cdot) \in R$. Then, the following system can be represented as a comparison system for the impulsive differential system (3):

$$\begin{cases} \dot{\zeta} = g(\zeta, t), \quad t \neq t_k \\ \zeta(t_k^+) = \psi_k(\zeta(t_k)) \\ \zeta(t_0^+) = \zeta_0 = V(p(0), 0) \geq 0 \end{cases}$$

Definition 5. *If the condition $\lim_{t \to T} |p_i(t) - \bar{p}(t)| = 0$ holds for all agents $i = 1, 2, \ldots, M$, where $\bar{p}(t)$ is the average state of the agents, the NMASs can achieve average consensus.*

Lemma 2. *[14] Let's consider two vectors, O and r, in R^m, where $O = (O_1, O_2, \ldots, O_m)^T$ and $r = (r_1, r_2, \ldots, r_m)^T$. We assume the existence of a matrix $D_i^- = I - D_i$, where D_i represents the i-th element of matrix D. If the condition $|r_i| \leq 1$ holds for all i, then we can conclude that the vector obtained by applying the saturation function, denoted as $sat(O)$, lies within the convex hull of the set $\{D_i O + D_i^- r : i \in \{1, 2, \ldots, 2^m\}\}$.*

Remark 2. *If $\|Qx\|_\infty \leq 1$, the saturated function $sat(Px)$ is bounded within the convex hull of the set $\{D_i Px + D_i^- Qx : i \in \{1, 2, \ldots, 2^m\}\}$. Suppose $0 \leq q_i \leq 1$ and $\sum_{i=1}^{2^m} q_i = 1$, the expression of $sat(Px)$ is equivalent to $sat(Px) = \sum_{i=1}^{2^m} q_i (D_i P + D_i^- Q)x$.*

Lemma 3. *[27]: Let $Z = \{Z_1, Z_2, \ldots, Z_m\}^T$. $L^{\sigma(t)}$ is a positive semi-definite matrix. The equation hold:*

$$Z^T L^{\sigma(t)} Z = \frac{1}{2} \sum_{i,j=1}^{m} a_{ij}^{\sigma(t)} (Z_i - Z_j)^2$$

Lemma 4. *[28]: Consider the non-negative value z_i, where $0 < \gamma < 1$. The following inequalities hold:*

$$\sum_{i=1}^{m} z_i^\gamma \geq \left(\sum_{i=1}^{m} z_i \right)^\gamma$$

Assumption 1. *There exists positive and known constants ϱ and D satisfying the following*

$$\|\Psi(\ell_i(t), t) - \Psi(\ell_j(t), t)\| = \varrho \|\ell_i(t) - \ell_j(t)\|$$

and

$$|d(p_i(t), t)| \leq D$$

Note: If the disturbance bound is time-varying but strictly bounded (i.e., $D(t) \leq D_{max}$), the theoretical stability remains valid by replacing D with D_{max}, though it increases the conservatism of the settling time Ω. If D is completely unknown, the strict fixed-time convergence cannot be guaranteed, which remains a limitation to be addressed by adaptive control in future work.

Assumption 2. *If there is an agent as the root node, and there exists a spanning tree in $G^{\sigma(t)}$, then $G^{\sigma(t)}$ is connected in all possible topologies $G_\mu^{\sigma(t)}$, $\mu \in S = \{1, 2, \cdots s\}$.*

3. Main Result

In this section, we introduce a state-constrained impulsive control strategy that incorporates a saturation function. This strategy is based on our investigation of FT consistency. Our control approach relies on FT theory, independent of the initial state, to ensure system stability and consistency at a fixed time. The primary objective is to limit the impulsive actions of agents and their neighboring agents, enabling NMASs with uncertain disturbances to achieve stability.

To achieve this goal, our control strategy is designed to implement FT control during non-impulsive intervals and apply saturation constraints during impulsive intervals. This approach guarantees system consistency under saturation constraints during FT. Here, we define the control protocol for designing NMASs composed of N agents.

$$u_i(t) = \begin{cases} c_1 \sum\limits_{j \in N_i} a_{ij}^{\sigma(t)} \text{sign}\left(p_j(t) - p_i(t)\right) - \varpi p_i(t) + c_2 \sum\limits_{j \in N_i} a_{ij}^{\sigma(t)} (p_j(t) - p_i(t))^m, \ t \neq t_k \\ sat\left(q_i\left(t\right)\right) \delta\left(t - t_k\right), \ t = t_k \end{cases} \tag{4}$$

Here, c_1 and c_2 are positive constants, and ϖ denotes the control gain constant. The control parameter plays a vital role in smoothing the consistency curve and improving the convergence rate of the smoothing system. The function $sign(\cdot)$ represents the sign function, and $sat(\cdot)$ refers to the saturation function. The variable d_k represents the impulsive gain at the k-th impulsive moment, while $\delta(t-t_k)$ denotes the Dirac delta function at time t_k. Specifically, the Dirac delta function takes the value of 1 when t is equal to t_k, and it is 0 at all other times.

Remark 3. *In order to achieve the goal, different control methods are used in the impulsive and non-impulsive moments, which will be compared in the Example 1 to demonstrate the necessity of combining the two types of control.*

Let's define an impulsive sequence in the system that satisfies the inequality $0 < t_0 < t_1 < \cdots < t_k$ and $\lim_{k\to\infty} t_k = +\infty$. The definitions are as follows: $\Delta p_i(t_k) = p_i(t_k^+) - p_i(t_k^-)$, where $p_i(t_k)$ represents the value of p_i at the impulsive moment t_k, $p_i(t_k^+)$ is the limit of p_i as t approaches t_k from the right, and $p_i(t_k^-)$ is the limit of p_i as t approaches t_k from the left.

Combining the node dynamics (2) with the proposed controller (4) yields the following closed-loop error system:

$$\begin{cases} \dot{p}_i(t) = c_1 \sum\limits_{j \in N_i} a_{ij}^{\sigma(t)} sign\left(p_j(t) - p_i(t)\right) + c_2 \sum\limits_{j \in N_i} a_{ij}^{\sigma(t)} (p_j(t) - p_i(t))^{\varepsilon} - \varpi p_i\left(t\right) \\ + f\left(p_i(t), t\right) + d\left(p_i(t), t\right), \qquad t \neq t_k \\ \Delta p_i(t_k) = sat\left(q_i\left(t\right)\right) \delta\left(t - t_k\right), t = t_k \end{cases} \tag{5}$$

where $q_i\left(t\right) = d_k \sum\limits_{j \in N_i} a_{ij}^{\sigma(t)} (p_j(t) - p_i(t)$. By Definition 5, the state error of the i-th agent can be denoted as $\varphi_i(t) = p_i(t) - \bar{p}(t)$, which is defined as the difference between the individual state $p_i(t)$ and the average state of the system $\bar{p}(t)$. Consequently, the system error can be expressed as follows:

$$\begin{cases} \dot{\varphi}_i(t) = c_1 \sum\limits_{j \in N_i} a_{ij}^{\sigma(t)} sign(\varphi_j(t) - \varphi_i(t)) \ - \varpi \varphi_i(t) + c_2 \sum\limits_{j \in N_i} a_{ij}^{\sigma(t)} (\varphi_j(t) - \varphi_i(t))^{\varepsilon} \\ \qquad + f\left(p_i(t), t\right) - \dfrac{1}{N} \sum\limits_{i=1}^{N} f\left(p_i\left(t\right), t\right) + d\left(p_i(t), t\right) - \dfrac{1}{N} \sum\limits_{i=1}^{N} d\left(p_i\left(t\right), t\right), t \neq t_k \\ \Delta \varphi_i\left(t_k\right) = \left[I_n - \dfrac{1 1^T}{n}\right] \times sat\left(d_k\left(-L^{\sigma(t)} \varphi\left(t_k^-\right)\right)\right), t = t_k \end{cases} \tag{6}$$

Theorem 1. *Under Assumptions 1–2 and the conditions stated in Definition 5, consider the NMASs (2) with uncertain disturbances. By implementing the control protocol (4), the system achieves FT consensus within a settling time Ω. Specifically, the following properties hold:*

(i) If $0 < \gamma < 1$, the value of the settling time Ω is determined as follows:

$$\Omega = \frac{\tau_{\max}}{(1-v)\ln\gamma} \ln\left[1 - \frac{\gamma^{1-v}\ln\gamma}{\bar{c}_2 \tau_{\max}}\right] + \frac{\tau_{\max}}{(1-u)\ln\gamma} \ln\left[\frac{\bar{c}_1 \tau_{\min}}{\bar{c}_1 \tau_{\min} - \gamma^{u-1}\ln\gamma}\right]$$

(ii) If $\gamma = 1$, the value of the settling time Ω is determined as follows:

$$\Omega = \frac{1}{\bar{c}_2\left(v-1\right)} + \frac{1}{\bar{c}_1\left(1-u\right)}$$

where the constants satisfy the following equations and inequalities:

$$\begin{cases} \bar{c}_1 = \dfrac{c_1 + 2\varrho}{(\lambda_2^{min}(L_2^{\sigma(t)}))^{\frac{1}{2}} + DN^{\frac{1}{2}}} \\ \bar{c}_2 = \dfrac{c_2 + 2\varrho}{2^m N^{1-m} (\lambda_2^{min}(L_{\frac{2}{1+\varepsilon}}^{\sigma(t)}))^{\frac{1+\varepsilon}{2}}} \\ \|[I+\theta]^T [I+\theta]\| \leq \gamma \end{cases}$$

where $\lambda_2^{min}\left(L^{\sigma(t)}\right) = min\left\{\lambda_2\left(L^{\sigma(t_0)}\right), \lambda_2\left(L^{\sigma(t_1)}\right), ...\right\}$, *and* $L_2^{\sigma(t)}$ *and* $L_{\frac{2}{1+\varepsilon}}^{\sigma(t)}$ *are the Laplacian matrices corresponding to* $\Lambda_1 = \left[a_{ij}{}^2\right]$ *and* $\Lambda_2 = \left[a_{ij}{}^{\frac{2}{1+\varepsilon}}\right]$, *respectively.* $\theta = (I - \frac{11^T}{N}) \max\limits_{i \in [1,2^m)} (d_k(D_i(-L^{\sigma(t)} + D_i^- Q))$, *and* $\|Hx\|_\infty \leq 1$.

Proof. The following Lyapunov function candidate is considered:

$$\Gamma(t) = \frac{1}{2} \sum_{i=1}^{N} \varphi_i^2(t) \tag{7}$$

At non-impulsive moments, when $t \neq t_k$, the expression for $\dot{\Gamma}(t)$ is as follows:

$$\begin{aligned} \dot{\Gamma}(t) \leq & \sum_{i=1}^{N} \varphi_i^T(t) \left[c_1 \sum_{j \in N_i} a_{ij}^{\sigma(t)} sign(\varphi_j(t) - \varphi_i(t)) \right] + \sum_{i=1}^{N} \varphi_i^T(t) \left[c_2 \sum_{j \in N_i} a_{ij}^{\sigma(t)} (\varphi_j(t) - \varphi_i(t))^m \right] \\ & + \sum_{i=1}^{N} \varphi_i^T(t) \left[f(p_i(t), t) - \frac{1}{N} \sum_{i=1}^{N} f(p_i(t), t) \right] + \sum_{i=1}^{N} \varphi_i^T(t) \left[d(p_i(t), t) - \frac{1}{N} \sum_{i=1}^{N} d(p_i(t), t) \right] \\ & - \varpi \sum_{i=1}^{N} \varphi_i^T(t) \varphi_i(t) \\ \leq & \frac{c_1}{2} \sum_{i=1}^{N} \sum_{j=1}^{N} a_{ij}^{\sigma(t)} [\varphi_i(t) - \varphi_j(t)] \times sign(\varphi_j(t) - \varphi_i(t)) \\ & + \frac{c_2}{2} \sum_{i=1}^{N} \sum_{j=1}^{N} a_{ij}^{\sigma(t)} [\varphi_i(t) - \varphi_j(t)] \times [\varphi_j(t) - \varphi_i(t)]^m \\ & + \sum_{i=1}^{N} \varphi_i(t) \left[f(p_i(t), t) - \frac{1}{N} \sum_{i=1}^{N} f(p_i(t), t) \right] + \sum_{i=1}^{N} \varphi_i(t) \left[d(p_i(t), t) - \frac{1}{N} \sum_{i=1}^{N} d(p_i(t), t) \right] \end{aligned} \tag{8}$$

By employing the conditions outlined in 1, the derivative $\dot{\Gamma}(t)$ can be upper-bounded by:

$$\begin{aligned} \dot{\Gamma}(t) \leq & -\frac{c_1}{2} \left[\sum_{i=1}^{N} \sum_{j=1}^{N} \left(a_{ij}^{\sigma(t)} \right)^2 |\varphi_i(t) - \varphi_j(t)|^2 \right]^{\frac{1}{2}} - \frac{c_2}{2} \left[\sum_{i=1}^{N} \sum_{j=1}^{N} \left(a_{ij}^{\sigma(t)} \right)^{\frac{2}{1+\varepsilon}} |\varphi_i(t) - \varphi_j(t)|^2 \right]^{\frac{1+\varepsilon}{2}} \\ & + \sum_{i=1}^{N} D |\varphi_i(t)| + \sum_{i=1}^{N} \rho |\varphi_i(t)|^2 \end{aligned} \tag{9}$$

According to Lemma 3, certain expressions in the above equation can be modified to the following form:

$$\sum_{i=1}^{N} \sum_{j=1}^{N} \left(a_{ij}^{\sigma(t)} \right)^2 |\varphi_i(t) - \varphi_j(t)|^2 2\varphi^T(t) L_2^{\sigma(t)} \varphi(t) \geq 4\lambda_2 \left(L_2^{\sigma(t)} \right) \Gamma(t) \tag{10}$$

and

$$\sum_{i=1}^{N} \sum_{j=1}^{N} \left(a_{ij}^{\sigma(t)} \right)^{\frac{2}{1+\varepsilon}} |\varphi_i(t) - \varphi_j(t)|^2 = 2\varphi^T(t) L_{\frac{2}{1+\varepsilon}}^{\sigma(t)} \varphi(t) \geq 4\lambda_2 \left(L_{\frac{2}{1+\varepsilon}}^{\sigma(t)} \right) \Gamma(t) \tag{11}$$

In the equation, the Laplacian matrix of the topological graph $G(\Lambda_2^{\sigma(t)})$ is denoted by $L_2^{\sigma(t)}$, and the Laplacian graph of $G(\Lambda_{\frac{2}{1+\varepsilon}}^{\sigma(t)})$ is represented by $L_{\frac{2}{1+\varepsilon}}^{\sigma(t)}$. Substituting the above inequality into Equation (9), one obtains the following inequality:

$$\begin{aligned}
\dot{\Gamma}(t) &\leq -\frac{c_1}{2}\left[4\lambda_2\left(L_2^{\sigma(t)}\right)\Gamma(t)\right]^{\frac{1}{2}} + 2\rho\Gamma(t) - \frac{c_2}{2}N^{1-m}\left[4\lambda_2\left(L_{\frac{2}{1+\varepsilon}}^{\sigma(t)}\right)\Gamma(t)\right]^{\frac{1+\varepsilon}{2}} + DN^{\frac{1}{2}}\left[\sum_{i=1}^{N} D|\varphi_i(t)|^2\right]^{\frac{1}{2}} \\
&= -c_1\left[\lambda_2\left(L_2^{\sigma(t)}\right)\Gamma(t)\right]^{\frac{1}{2}} + D(N)^{\frac{1}{2}}\Gamma^{\frac{1}{2}}(t) - c_2 2^m N^{1-m}\left[\lambda_2\left(L_{\frac{2}{1+\varepsilon}}^{\sigma(t)}\right)\Gamma(t)\right]^{\frac{1+\varepsilon}{2}} + 2\rho\Gamma(t) \\
&= -c_1\left(\lambda_2\left(L_2^{\sigma(t)}\right)^{\frac{1}{2}} + D(N)^{\frac{1}{2}}\right)\Gamma^{\frac{1}{2}}(t) - c_2 2^m N^{1-m}\left[\lambda_2\left(L_{\frac{2}{1+\varepsilon}}^{\sigma(t)}\right)\right]^{\frac{1+\varepsilon}{2}}\Gamma^{\frac{1+\varepsilon}{2}}(t) + 2\rho\Gamma(t) \\
&\leq 2\rho\left(\Gamma(t) - \Gamma^{\frac{1}{2}}(t) - \Gamma^{\frac{1+\varepsilon}{2}}(t)\right) - \bar{c}_1\Gamma^u(t) - \bar{c}_2\Gamma^v(t)
\end{aligned} \tag{12}$$

Considering the condition $\Gamma(t) > 0$, we can observe that the inequality $\Gamma(t) - \Gamma(t)^{\frac{1}{2}} - \Gamma(t)^{\frac{1+\varepsilon}{2}} < 0$ holds. By setting $u = \frac{1}{2}$ and $v = \frac{1+\varepsilon}{2}$, the derivative of the Lyapunov function as a whole can be expressed by the following inequality:

$$\dot{\Gamma}(t) < -\bar{c}_1\Gamma^u(t) - \bar{c}_2\Gamma^v(t) \tag{13}$$

At the impulsive moment $t = t_k$, Lemma 2 and Remark 2 can be utilized to construct the Lyapunov function for the system as follows:

$$\begin{aligned}
\Gamma(t_k) &= \frac{1}{2}\varphi^T(t_k^+)\varphi(t_k^+) \\
&= \frac{1}{2}[(I + (I - \frac{11^T}{N})Sat(d_k(-L_{\sigma(t)}\varphi(t_k^-))))]^T [(I + (I - \frac{11^T}{N})Sat(d_k(-L_{\sigma(t)}\varphi(t_k^-))))] \\
&\leq \frac{1}{2}\varphi^T(t_k^-)\varphi(t_k^-)(I+\theta)^T(I+\theta) \\
&\leq \gamma\Gamma(t_k^-)
\end{aligned} \tag{14}$$

where $\theta = (I - \frac{11^T}{N}) \max\limits_{i\in[1,2^m)}(d_k(D_i(-L^{\sigma(t)} + D_i^- Q))$. Based on equations (16) and (17) above, this can be further summarised as follows:

$$\begin{cases}
\dot{\Gamma}(t) \leq -\bar{c}_1\Gamma^u(t) - \bar{c}_2\Gamma^v(t), t \neq t_k \\
\Gamma\left(t_k^+\right) \leq \gamma\Gamma\left(t_k^-\right), t = t_k
\end{cases} \tag{15}$$

According to Definition 4, it can be inferred that the Equation (15) can be expressed in the form of the following comparison system:

$$\begin{cases}
\dot{\eta}(t) = \begin{cases} -\bar{c}_2\Gamma^v(t), \ \eta \geq 1, \ t \neq t_k \\ -\bar{c}_1\Gamma^u(t), \ 0 < \eta < 1, \ t \neq t_k \end{cases} \\
\eta(t_k) = \gamma\eta\left(t_k^-\right), \ t = t_k \\
\eta(0) = \eta_0 = \dfrac{1}{2}\varphi^T(0)\varphi(0)
\end{cases} \tag{16}$$

By comparing equations (15) and (16), we can conclude that $0 < \Gamma(t) < \eta(t)$. As a result, if there exists a value $\Omega > 0$ such that $\eta(t) \equiv 0$, then it follows that $\Gamma(t) \equiv 0$ for $t > \Omega$. When the condition $\eta(t) \equiv 0$ is met, the variable $\Gamma(t)$ remains at zero after a certain time point Ω. In summary, whether the error system (6) can reach stability at a fixed time can be transformed into whether the corresponding comparison system (16) has a zero solution.

Remark 4. *The comparative systems analysis method plays a vital role in the theory of impulsive differential equations. Its most significant advantage lies in simplifying the system model, transforming a complex set of nonlinear analytical equations into a scalar set of nonlinear equations. By discussing the consistency of NMASs from different perspectives, this method significantly reduces the complexity of the theoretical analysis of the system.*

Next, the system (16) will be discussed in two cases: $0 < \gamma < 1$ and $\gamma = 1$. Firstly, let's consider the case

when $0 < \gamma < 1$. Assuming $\lambda(t) = \eta^{1-v}(t)$ when $\eta(t) \geq 1$, it can be observed from system (16) that $\lambda(t) \to 0$ as $\eta(t) \to \infty$, and $\lambda(t) \to 1$ as $\eta(t) \to 1$. Thus, the system (16) can be expressed as follows:

$$\begin{cases} \dot{\lambda}(t) = (v-1)\,\bar{c}_2,\ 0 < \lambda \leq 1,\ t \neq t_k \\ \lambda(t_k) = \bar{\gamma}\lambda\left(t_k^-\right),\ t = t_k \\ \lambda(0) = \lambda_0 = \eta^{1-v} \end{cases} \tag{17}$$

where $\bar{\gamma} = \gamma^{1-v}$, and $\bar{\gamma} > 1$. Based on knowledge of the relevant inequality theory [29], the Equation (17) can be computed as

$$\lambda(t) = \bar{\gamma}^{N(0,t)}\lambda(0) + (v-1)\,\bar{c}_2 \int_0^t \bar{\gamma}^{N(s,t)} ds \tag{18}$$

Since $\lambda(0) = \bar{\gamma}^{N(0,0)}\lambda(0) = \lambda_0 < 1$ and $\lim_{t\to\infty} \lambda(t) \to \infty$. Thus, $\lambda(t)$ is a monotonically increasing function on the interval $[0, \infty)$. Furthermore, when $0 < t < \Omega_1$, there exists a time Ω_1 satisfying $\lim_{t\to\Omega_1} \lambda(t) \to 1$ and $0 < \lambda < 1$. Thus, further calculations based on Equation (19) lead to

$$\bar{\gamma}^{N(0,t)}\lambda(0) + (v-1)\,\bar{c}_2 \int_0^t \bar{\gamma}^{N(s,t)} ds = 1 \tag{19}$$

According to Equation (17), from which it can be deduced that

$$(v-1)\,\bar{c}_2 \int_0^t \bar{\gamma}^{N(s,t)} ds \leq 1 \tag{20}$$

Next, the inequalities $\frac{t-s}{\tau_{\max}} - 1 \leq N(s,t)$ and $\bar{\gamma} = \gamma^{1-v}$ in Assumption 2 lead to the following inequalities:

$$t \leq \frac{\tau_{\max}}{\ln \bar{\gamma}} \ln\left[1 - \frac{\bar{\gamma}\ln\bar{\gamma}}{\bar{c}_2\,(1-v)\,\tau_{\max}}\right] = \Omega_1 \tag{21}$$

Since $\bar{\gamma} = \gamma^{1-v}$, the resulting inequality (21) above can be further transformed into

$$\Omega_1 = \frac{\tau_{\max}}{(1-v)\ln\gamma} \ln\left[1 - \frac{\gamma^{1-v}\ln\gamma}{\bar{c}_2\tau_{\max}}\right] \tag{22}$$

Summing up, one obtains that the solution (17) reaches 1 at a fixed time Ω_1. Next, similar to the analysis above, when $0 \leq \eta(t) < 1$, suppose that $\lambda(t) = \eta^{1-u}(t)$. From system (19), we can deduce that as $\eta(t) \to 1$, the variable $\lambda(t) \to 1$, and as $\eta(t) \to 0$, $\lambda(t) \to 0$. Thus, the comparison system (16) can be further expressed as

$$\begin{cases} \dot{\lambda}(t) = -(1-u)\,\bar{c}_1,\ 0 < \lambda \leq 1,\ t \neq t_k \\ \lambda(t_k) = \tilde{\gamma}\lambda\left(t_k^-\right),\ t = t_k \\ \lambda(0) = 1 \end{cases} \tag{23}$$

where $\tilde{\gamma} = \gamma^{1-u}$, $0 < \tilde{\gamma} < 1$, and when $\eta(t) \to 0$ is equivalent to $\lambda(t) \to 0$. Therefore, the equation as mentioned earlier can be simplified and calculated as follows:

$$\lambda(t) = \tilde{\gamma}^{N(0,t)}\lambda(0) - (1-u)\,\bar{c}_1 \int_0^t \tilde{\gamma}^{N(s,t)} ds \tag{24}$$

Since $0 < \tilde{\gamma} < 1$, then $\tilde{\gamma}^{\frac{t-s}{\tau_{\min}}} < \tilde{\gamma}^{N(s,t)} < \tilde{\gamma}^{\frac{t-s}{\tau_{\max}}-1}$, and $\lambda(0) = 1$ and $\lambda(t) = 0$. Thus, it can be deduced from the calculation that

$$\begin{aligned} \lambda(t) &= \tilde{\gamma}^{N(0,t)}\lambda(0) - (1-u)\,\bar{c}_1 \int_0^t \tilde{\gamma}^{N(s,t)} ds \\ &\leq \tilde{\gamma}^{\frac{t}{\tau_{\max}}-1} - (1-u)\,\bar{c}_1 \int_0^t \tilde{\gamma}^{\frac{t}{\tau_{\min}}} ds \\ &\leq \left[\tilde{\gamma}^{-1} - (1-u)\,\bar{c}_1 \frac{\tau_{\min}}{\ln\tilde{\gamma}}\right] \tilde{\gamma}^{\frac{t}{\tau_{\max}}} + (1-u)\,\bar{c}_1 \frac{\tau_{\min}}{\ln\tilde{\gamma}} \end{aligned} \tag{25}$$

Eventually, based on Equation (25), we can deduce that $\lambda(0) > 0$, $\lambda(+\infty) < 0$, and $\dot{\lambda}(t) < 0$. Therefore, there exists a positive time Ω_2 such that $\lambda(\Omega_2) = 0$, indicating the convergence of the system from 1 to 0. The duration required for the system to achieve this convergence can be expressed as follows:

$$\Omega_2 = \frac{\tau_{\max}}{(1-u)\ln\gamma} \ln\left[\frac{\bar{c}_1\tau_{\min}}{\bar{c}_1\tau_{\min} - \gamma^{u-1}\ln\gamma}\right] \tag{26}$$

Thus, when $0 < \gamma < 1$, the error system (6) for NMASs can be consistent for a fixed time $\Omega = \Omega_1 + \Omega_2$.

$$\Omega = \frac{\tau_{\max}}{(1-v)\ln\gamma} \ln\left[1 - \frac{\gamma^{1-v}\ln\gamma}{\bar{c}_2\tau_{\max}}\right] + \frac{\tau_{\max}}{(1-u)\ln\gamma} \ln\left[\frac{\bar{c}_1\tau_{\min}}{\bar{c}_1\tau_{\min} - \gamma^{u-1}\ln\gamma}\right] \tag{27}$$

Next, consider the second case $\gamma = 1$, then $\bar{\gamma} = \tilde{\gamma} = 1$, which can be computationally deduced from Equation (17) as follows:

$$\Omega_1 = \frac{1}{\bar{c}_2(v-1)} \tag{28}$$

Since $\lambda(0) = 1$ and $\lambda(t) = 0$, it can be obtained from Equation (23) that

$$\Omega_2 = \frac{1}{\bar{c}_1(1-u)} \tag{29}$$

The system described by Equation (6) can converge to zero at a fixed time Ω, irrespective of its initial value.

$$\Omega = \frac{1}{\bar{c}_2(v-1)} + \frac{1}{\bar{c}_1(1-u)} \tag{30}$$

This implies that the system's behavior becomes independent of its initial position after a finite time and for $t > \Omega$, $\Gamma(t) = 0$. To summarize, the presented evidence and findings establish the ability of the non-linear NMASs described by Equation (2) to attain a consensus within a fixed time, even in the presence of uncertain disturbances. □

Remark 5. *When $\gamma > 1$, then $\tilde{\gamma} > 1$, and as time t tends to infinity, the equation $\lambda(t) = \tilde{\gamma}^{N(0,t)}\lambda(0) - (1-u)\bar{c}_1\int_0^t \tilde{\gamma}^{N(s,t)}ds$ cannot converge from 1 to 0. Therefore, the system cannot stabilize at a fixed time Ω_2.*

Remark 6. *The above analysis shows that the comparative system (19) can be discussed in two parts. The first part is that Equation (20) converges to 1 at a fixed time Ω_1. The second part is that Equation (23) connects to 0 at a specified time Ω_2. Therefore, the time the system finally reaches consistency is $\Omega = \Omega_1 + \Omega_2$.*

Remark 7. *The comparative systems analysis approach plays a crucial role in the theory of impulsive differential equations. One of its most notable advantages is its capability to simplify the system model. This approach enables the transformation of complex systems with nonlinear analytical equations into scalar systems of nonlinear equations, making them more amenable to analysis. It also enables the discussion of the problem of NMASs consistency from different perspectives, significantly reducing the complexity of the theoretical analysis of the system.*

Corollary 1. *Based on Theorem 1 and Definition 3, the NMASs can achieve consensus with SMSTs in time Ω if $\sigma(t)$ is a semi-Markovian process, where Ω is set as follows:*

(i) If $0 < \gamma < 1$, the value of the settling time Ω is determined as follows:

$$\Omega = \frac{\tau_{\max}}{(1-v)\ln\gamma} \ln\left[1 - \frac{\gamma^{(1-v)\sum_{\mu\in S}\frac{\pi_\mu}{m_\mu}}\ln\gamma}{\bar{c}_2\tau_{\max}}\right] + \frac{\tau_{\max}}{(1-u)\ln\gamma} \ln\left[\frac{\bar{c}_1\tau_{\min}}{\bar{c}_1\tau_{\min} - \gamma^{(u-1)\sum_{\mu\in S}\frac{\pi_\mu}{m_\mu}}\ln\gamma}\right]$$

(ii) If $\gamma = 1$, the value of the settling time Ω is determined as follows:

$$\Omega = \frac{1}{\bar{c}_2(v-1)} + \frac{1}{\bar{c}_1(1-u)}$$

Proof. The proof is similar to Theorem 1. □

Remark 8. *Let $\widetilde{N}(s,t)$ denote the number of impulsive that occur during the time interval (s,t) when the topological topology is μ. In a semi-Markovian process, the duration of each topology is an exponentially distributed random variable. Thus, the total time spent in topology μ during the interval (s,t) follows an exponential distribution with parameter $1/m_\mu$, i.e., $\tau \sim exp(1/m_\mu)$. Therefore, the proportion of time spent in topology μ during the interval (s,t) is $\frac{t-s}{m_\mu}$.*

Remark 9. *This prostate explores the problem of achieving consensus in NMASs with SMSTs, considering the presence of random disturbances and other effects. It addresses the challenge of designing systems capable of coping with disturbances arising from arbitrary switching topologies. In contrast to previous investigations [14, 22–25] wherein instability was attributed to different factors, this paper elucidates that the instability herein stems from the SMSTs, where each graph corresponds to a distinct state within a Markovian process topology.*

4. Simulation

This section presents a series of numerical simulation experiments aimed at simulating and validating the feasibility and accuracy of the theoretical analysis. Firstly, this paper uses an undirected communication topology connection to avoid the issue of directed loops in the directed topology diagram leading to the system getting stuck in a dead loop, affecting the communication exchange between agents. It proposes three undirected communication topologies containing six agents, G_1, G_2, and G_3, as shown in Figure 1. The following are the Laplacian matrices associated with three distinct communication topologies.

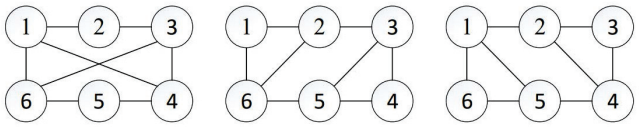

Figure 1. Different communication topologies for six agents of G_1,G_2,G_3.

$$\tilde{L}_1 = \begin{bmatrix} 3 & -1 & 0 & -1 & 0 & -1 \\ -1 & 2 & -1 & 0 & 0 & 0 \\ 0 & -1 & 3 & -1 & 0 & -1 \\ -1 & 0 & -1 & 3 & -1 & 0 \\ 0 & 0 & 0 & -1 & 2 & -1 \\ -1 & 0 & -1 & 0 & -1 & 3 \end{bmatrix} \quad \tilde{L}_2 = \begin{bmatrix} 2 & -1 & 0 & 0 & 0 & -1 \\ -1 & 3 & -1 & 0 & 0 & -1 \\ 0 & -1 & 3 & -1 & -1 & 0 \\ 0 & 0 & -1 & 2 & -1 & 0 \\ 0 & 0 & -1 & -1 & 3 & -1 \\ -1 & 0 & -1 & 0 & -1 & 3 \end{bmatrix} \quad \tilde{L}_3 = \begin{bmatrix} 3 & -1 & 0 & 0 & -1 & -1 \\ -1 & 3 & -1 & -1 & 0 & 0 \\ 0 & -1 & 2 & -1 & 0 & 0 \\ 0 & -1 & -1 & 3 & -1 & 0 \\ -1 & 0 & 0 & -1 & 3 & -1 \\ -1 & 0 & 0 & 0 & -1 & 2 \end{bmatrix}$$

The nonlinear function is set as

$$f(p_i(t), t) = 0.2 - 0.6\sin(p_i(t), t).$$

Setting the initial value as $p(0) = \{5, -3, 0.9, -2, 4, 2\}$, the uncertainty disturbance as $d(p_i(t), t) = 0.1\cos(p_i(t), t)$, it can be observed that $d(p_i(t), t)$ satisfies the conditions in Assumption 1 with $D = 0.1$. The switching signal $\sigma(t) = \mathrm{mod}(n, 2) + 2$, the impulsive gain and impulsive interval of the system control protocol is $d_k = 0.5$, $\Delta T = 0.02$, and the parameters for the system are set to $c_1 = 3$, $c_2 = 3$, $\rho = 0.3$, $m = 7/5$ and $\gamma = 0.9$, the matrix $Q = diag(-0.1, -0.3, -0.1, -0.2, -0.5, -0.1)$.

It is then calculated that $\|I + \theta\|^T \|I + \theta\|_{\max} = 0.8735 < \gamma$, and according to Theorem 1, the convergence time for the system (2) to reach consistency can be calculated as $\Omega = 3.6532s$.

The dynamic trajectories and the corresponding tracking errors are plotted in Figure 2a,b, verifying the efficacy of the formulated methodology (4).These results show that the error values converge to zero at time $T = 0.40s$. Based on this, we can conclude that the considered NMASs described in Equation (2) can achieve consensus using the proposed control strategy defined in Equation (4) under switching topologies.

When the initial states are $p(0) = \{-2, 6, -1, 5, -3, 4\}$, the state evolution diagrams and error evolution diagrams of NMASs are shown in Figure 2c,d. By comparing with the state diagrams in Figure 2a,b, it can be seen that the NMASs reach consistency in the same convergence time for two different initial states. This further shows that the convergence time of the FT consistency control protocol is independent of the initial state, thus solving the problem that the initial state is challenging to obtain and ensuring that the NMASs can reach consistency in a shorter time.

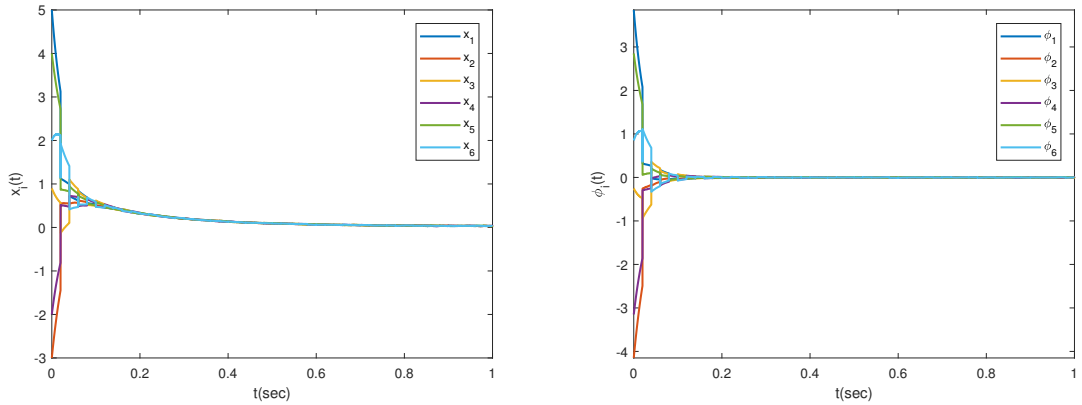

(a) state evolution

(b) error evolution

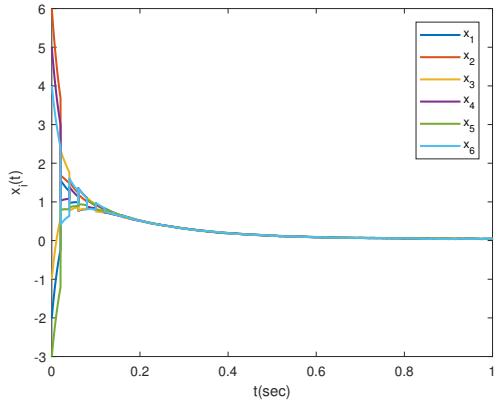

(c) state evolution

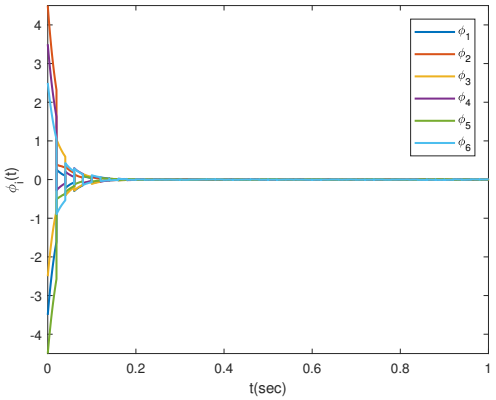

(d) error evolution

Figure 2. State and error evolution of six agents with the initial values $\{5, -3, 0.9, -2, 4, 2\}$ and $\{-2, 6, -1, 5, -3, 4\}$.

In practical applications, it is crucial to consider the design of constraints on the impulsive values of the controller, as evident from Figure 3a,b, the transient impulsive in Figure 3c exhibits significant variations, leading to large fluctuations in the system during operation. This instability harms the system's stability, thus irreversibly affecting the consistency and convergence of NMAS. Therefore, applying saturation constraints to the impulsive input is highly necessary. To better demonstrate the constraint on the impulsive timing input in this experiment, Figure 3c,f are presented, representing the saturated input and regular input at the impulsive timing for the same system. It can be observed that the constraint effect in this experiment is highly pronounced.

To further verify the superiority of the control strategy proposed in this paper relative to the single control strategy, the state and error evolution of Figures 4 and 5 show that under the impulsive protocol (31) with a single state constraint, consistency cannot be achieved within 0 to 4 s due to the short action time of the control method and the restricted instantaneous impulsive value. The system needs more time to achieve consistency in order to obtain stability.

$$u_i(t) = \begin{cases} sat\left(d_k \sum\limits_{j \in N_i} a_{ij}^{\sigma(t)} \left(p_j(t) - p_i(t)\right) \delta\left(t - t_k\right)\right), t = t_k \\ 0, t \neq t_k \end{cases} \tag{31}$$

Moreover, as shown in the error evolution diagram in Figure 5, the system can be stabilized at about the same time as the FT consistency control strategy if only a single control strategy (4) is considered.

$$u_i(t) = c_1 \sum_{j \in N_i} a_{ij}^{\sigma(t)} sign(p_j(t) - p_i(t)) + c_2 \sum_{j \in N_i} a_{ij}^{\sigma(t)} (p_j(t) - p_i(t))^m - \varpi p_i(t) \tag{32}$$

However, the continuous control approach leads to a significant increase in the communication cost of the system.

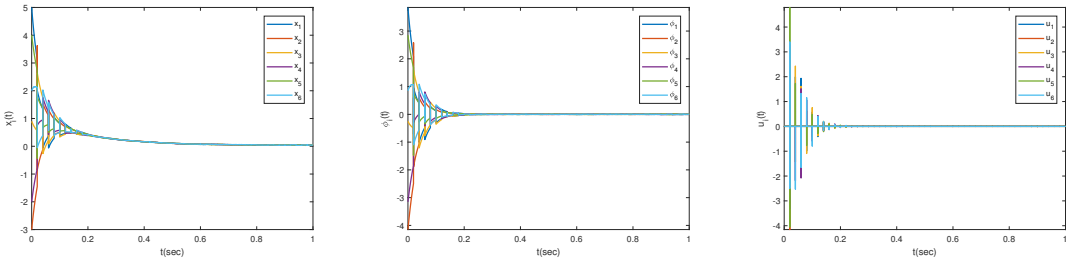

(a) state evolution (b) error evolution (c) control evolution

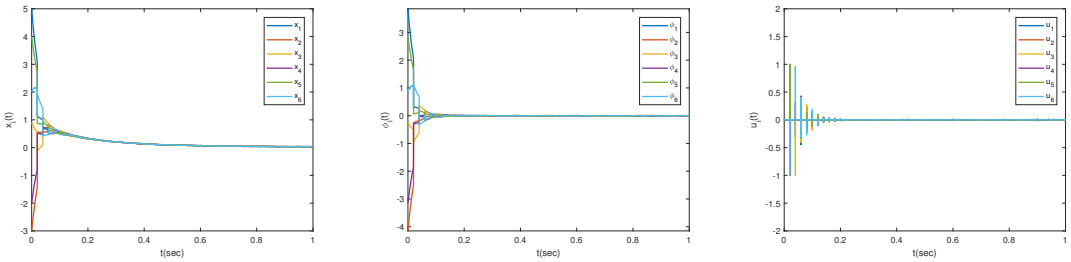

(d) state evolution (e) error evolution (f) control evolution

Figure 3. State evolution, error evolution, and control evolution in non-impulsive period of six agents without saturation constraint and with saturation constraint.

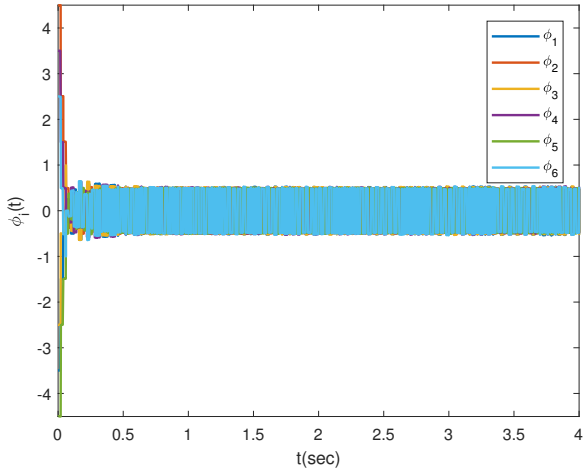

Figure 4. Error evolution of six agents with pure saturation constraint under switching topologies.

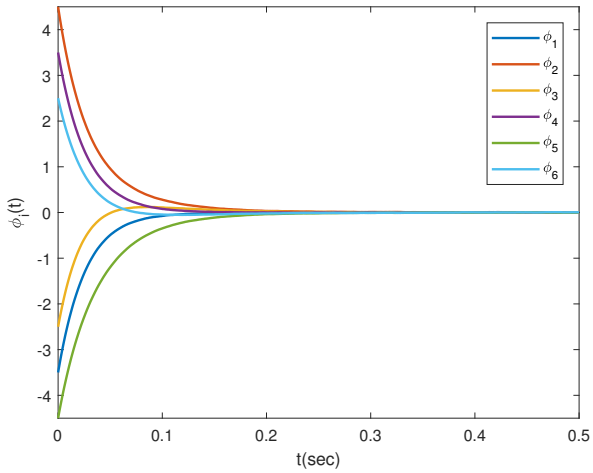

Figure 5. Error evolution of six agents with pure fixed time protocol under switching topologies.

This approach differs from Markovian switching topologies, which assume exponential distribution for dwell times and constant transition rates between any two topologies.

In comparison to Example 1, the predefined parameters remain essentially unchanged. However, in this case, the switching signal function $\sigma(t)$ is set as a semi-Markovian chain process. The set of states is denoted as $S = \{1, 2, 3\}$. The expected durations of topology dwell time are given as $m_1 = 0.015$, $m_2 = 0.012$, and $m_3 = 0.02$. Additionally, the transition probability matrix is represented by Π as follows:

$$\Pi = \begin{bmatrix} 0.2 & 0.3 & 0.5 \\ 0.5 & 0.2 & 0.3 \\ 0.3 & 0.5 & 0.2 \end{bmatrix}$$

This configuration enables a more realistic representation of the system dynamics and topology transitions.

Given the communication topology illustrated in Figure 1, with parameters $\tau_{\min} = 0.01$ and $\tau_{\max} = 0.03$ as defined in Definition 3, the convergence time required for achieving consensus, as per Corollary 1, is determined to be $\Omega = 2.3524s$. The switching dynamics of the communication topology are governed by a semi-Markov process $\sigma(t)$, which stochastically transitions between the topologies $\{G_1, G_2, G_3\}$. In such a system, inter-agent communication is influenced by both the present topology and the duration spent by the system in each topology state. To emulate the system's inherent randomness more faithfully, in Example 2, distinct durations are assigned to each topology graph, as illustrated in Figure 6c, offering a more nuanced depiction of the system's dynamics.

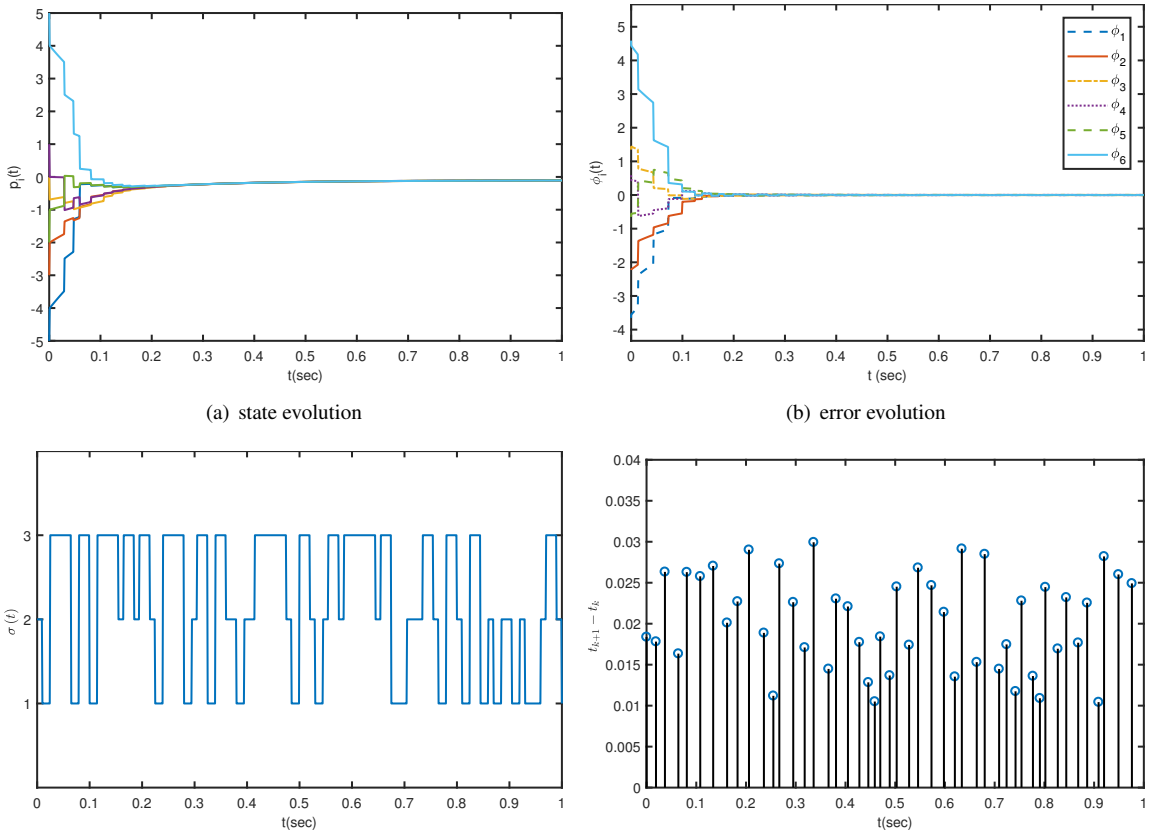

(a) state evolution (b) error evolution

(c) switching topologies (d) impulsive control signal

Figure 6. State evolution of six agents with saturation constraint under SMSTs.

To further imbue flexibility into impulsive scheduling and reflect the system's stochastic nature, impulsive intervals are randomized within a specified range while maintaining consistent upper and lower bounds. Figure 6d showcases this constraint, with impulsive intervals confined between 0.01 to 0.03.

Within this framework of semi-Markov chain topology switching, the multi-agent system ultimately converges towards consensus state, as evidenced by Figure 6a, effectively achieving average consensus, as demonstrated in Figure 6b.

To thoroughly assess the efficacy of the control strategy proposed in this paper, we conducted a series of

comparative experiments juxtaposed with a seminal work by authors referenced as [6]. In their study, [6] employed event-triggered continuous control techniques to attain FT consensus among non-continuous first-order multi-agent systems, even in the presence of disturbances. To enable a direct comparison, we applied both the control methodologies to a semi-Markov switching topology, employing the same multi-agent system as the experimental platform.

Our experimental findings unequivocally demonstrate the superior performance of the control strategy introduced in this paper. Notably, when comparing convergence rates, as depicted in Figure 7b against Figure 7a, our proposed strategy exhibits significantly faster convergence dynamics than that of [6]. Furthermore, in contrast to the continuous control paradigm employed by [6], our discontinuous control strategy, depicted in Figure 8a, triggers fewer pulses, thereby conserving system resources.

However, despite these advantages, it's imperative to acknowledge a slight trade-off in stability. As illustrated in Figure 9b compared to Figure 9a from [6], our strategy, incorporating disparate controls at varying instants and influenced by the sign function, exhibits marginally less satisfactory stability characteristics.

The strategy proposed here redefines the boundary between convergence speed and resource economy, consistently outstripping traditional benchmarks. Nevertheless, the symbiotic link between control design and stability remains a complex frontier. This study highlights that the path to true optimization is context-dependent, requiring a strategic alignment of control parameters to meet the rigorous demands of real-world operations.

Ultimately, the evidence suggests that relying on a single control paradigm is no longer sufficient for the rigors of modern NMASs. By weaving together a discontinuous state-constrained impulsive protocol with a FT consistency scheme, we've moved beyond simple incremental improvements. This fusion creates a unique synergy: it aggressively prunes communication overhead while fortifying the system's stability against the unpredictability of its starting point. It is this specific architectural balance that transforms theoretical consistency into a deployment-ready reality.

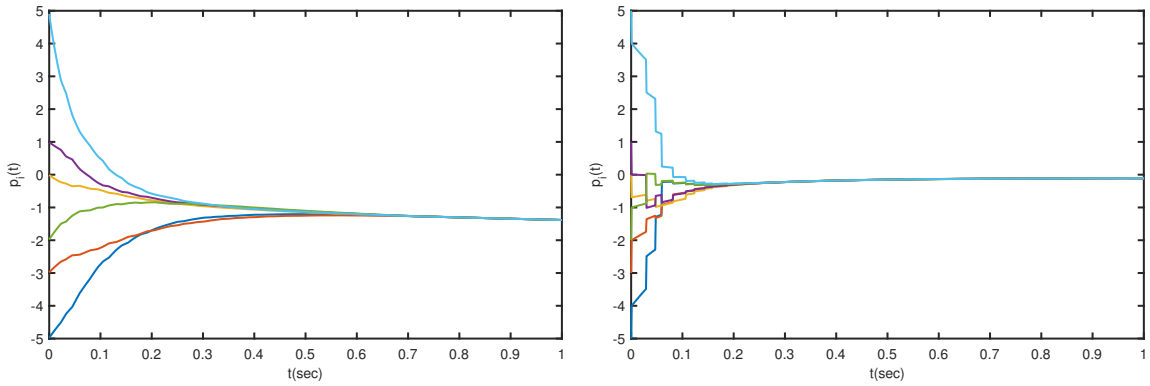

(a) state evolution of [6] (b) state evolution

Figure 7. State evolution of six agents with a saturation constraint under SMSTs with different theories: (**a**) the theory of [6]; (**b**) Corollary 1.

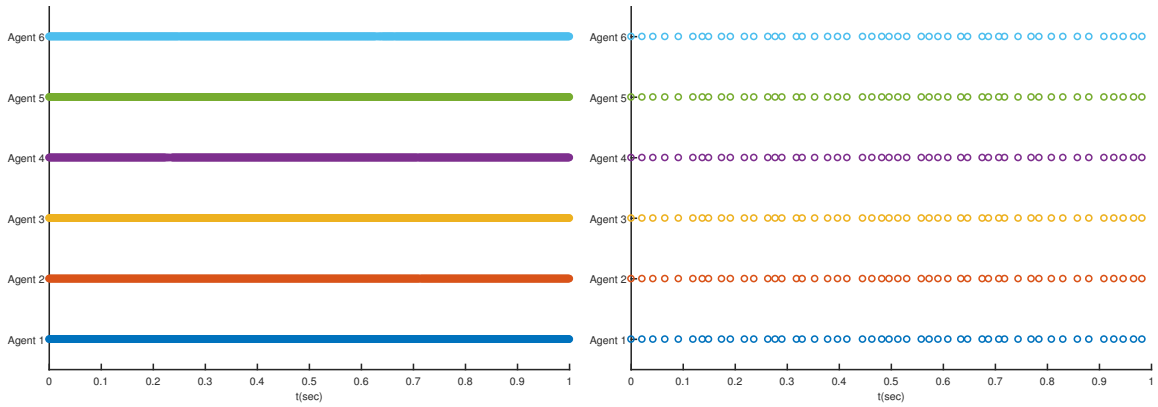

(a) event triggered instants of [6] (b) impulsive instants

Figure 8. Trigger instants of six agents with a saturation constraint under SMSTs with different theories: (**a**) the theory of [6]; (**b**) Corollary 1.

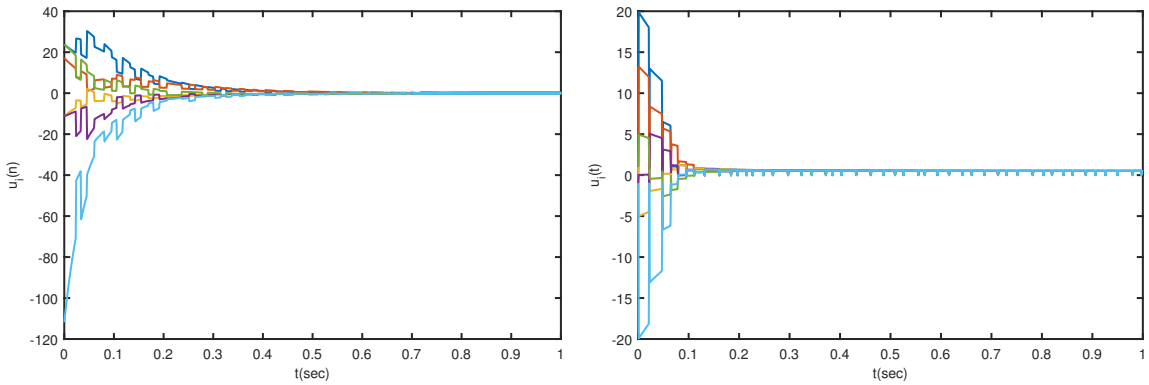

(a) control evolution of [6] (b) control evolution

Figure 9. Control evolution of six agents with saturation constraint under SMSTs with different theories: (**a**) the theory of [6]; (**b**) Corollary 1.

5. Conclusions

This paper has focused on the FT consensus of NMASs with uncertain disturbances under state-constrained impulsive control. To better approximate real-world situations, the study has considered indefinite disturbances and has incorporated FT interval switching topologies alongside SMSTs. Compared with traditional finite-time control approaches, using the FT consensus control protocol has made it possible to achieve consensus at any initial state, thus solving the problem of obtaining precise initial states for convergence. Furthermore, in contrast to existing continuous control or standard impulsive methods that may cause resource inefficiency or transient instability, a novel state-constrained impulsive control strategy has been designed in conjunction with the FT control strategy. This approach effectively restricts large fluctuations while reducing communication burdens. Sufficient conditions for achieving consensus convergence in the system have been derived, and the paper has proven that the NMASs with uncertain disturbances can be effectively controlled under state-constrained impact control. Finally, it should be noted that for practical applications, the assumptions regarding the connection between agents and the type of uncertain disturbances have remained still conservative, which points out the direction for future research.

Author Contributions

S.Y.: Conceptualization, Methodology, Formal Analysis, Writing—Original Draft; L.Z.: Data Curation, Writing—Original Draft; J.W.: Data Curation, Writing—Review and Editing; X.J.: Software, Validation; L.J.: Funding Acquisition, Resources, Supervision. All authors have read and agreed to the published version of the manuscript.

Funding

This work was supported by the National Natural Science Foundation of China (Grants 62006031, 62276036, 61876200),in part by the Project of Scientific and Technological Research Program of Chongqing Municipal Education Commission under Grant No. KJZD-202300624.

Institutional Review Board Statement

Not applicable.

Informed Consent Statement

Not applicable.

Data Availability Statement

The datasets generated or analyzed during this study are available from the corresponding author on reasonable request.

Conflicts of Interest

The authors declare no conflict of interest.

Use of AI and AI-assisted Technologies

No AI tools were utilized for this paper.

References

1. Zhou, C.; Wang, Y.; Lv, M.; et al. Neural-Adaptive Specified-Time Constrained Consensus Tracking Control of High-Order Nonlinear Multi-Agent Systems with Unknown Control Directions and Actuator Faults. *Neurocomputing* **2023**, *538*, 126168.
2. Fei, Y.; Shi, P.; Lim, C.C. Neural-Based Formation Control of Uncertain Multi-Agent Systems with Actuator Saturation. *Nonlinear Dyn.* **2022**, *108*, 3693–3709.
3. Ren, H.; Wang, Y.; Liu, M.; et al. An Optimal Estimation Framework of Multi-Agent Systems with Random Transport Protocol. *IEEE Trans. Signal Process.* **2022**, *70*, 2548–2559.
4. Wang, Y.W.; Zhang, Y.; Liu, X.K.; et al. Distributed Predefined-time Optimization and Control for Multi-bus DC Microgrid. *IEEE Trans. Power Syst.* **2024**, *39*, 5769–5779.
5. Wang, Y.W.; Lei, Y.; Bian, T.; et al. Distributed Control of Nonlinear Multiagent Systems with Unknown and Nonidentical Control Directions via Event-Triggered Communication. *IEEE Trans. Cybern.* **2019**, *50*, 1820–1832.
6. Guo, Y.; Tian, Y.; Ji, Y.; et al. Fixed-time Consensus of Nonlinear Multi-Agent System with Uncertain Disturbances Based on Event-Triggered Strategy. *ISA Trans.* **2022**, *126*, 629–637.
7. Li, K.; Xu, Y.; Li, Y. Data-Based Event-Triggered Cooperative Optimal Output Regulation of Nonlinear Multiagent Systems. *IEEE Trans. Syst. Man, Cybern. Syst.* **2025**, *55*, 6273 – 6284.
8. Ma, T.; Li, K.; Zhang, Z.; et al. Impulsive Consensus of One-Sided Lipschitz Nonlinear Multi-Agent Systems with Semi-Markov Switching Topologies. *Nonlinear Anal. Hybrid Syst.* **2021**, *40*, 101020.
9. Hu, Z.; Mu, X. Impulsive Consensus of Stochastic Multi-Agent Systems under Semi-Markovian Switching Topologies and Application. *Automatica* **2023**, *150*, 110871.
10. Yu, Z.; Wang, X.; Zhong, S.; et al. Impulsive Control for One-Side Lipschitz Nonlinear MASs under Semi-Markovian Switching Topologies with Partially Unknown Transition Probabilities. *Nonlinear Anal. Hybrid Syst.* **2023**, *48*, 101336.
11. Li, L.; Li, C.; Li, H. Fully State Constraint Impulsive Control for Non-Autonomous Delayed Nonlinear Dynamic Systems. *Nonlinear Anal. Hybrid Syst.* **2018**, *29*, 383–394.
12. Li, L.; Li, C.; Zhang, W. Delayed-Impulsive Control for Difference Systems with Actuator Saturation and Its Synchronisation Application. *IET Control. Theory Appl.* **2019**, *13*, 1129–1136.
13. Li, L.; Li, C.; Li, H. An Analysis and Design for Time-Varying Structures Dynamical Networks via State Constraint Impulsive Control. *Int. J. Control.* **2019**, *92*, 2820–2828.
14. Wang, J.; Yang, S.; Wang, Q.; et al. Finite-Time Consensus of Nonlinear Delayed Multi-Agent System via State-Constraint Impulsive Control under Switching Topologies. *Nonlinear Dyn.* **2023**, *111*, 12267–12281.
15. Liu, Y.J.; Shang, X.; Tang, L.; et al. Finite-Time Consensus Adaptive Neural Network Control for Nonlinear Multiagent Systems Under PDE Models. *IEEE Trans. Neural Netw. Learn. Syst.* **2024**, *36*, 6218–6228.
16. Ma, Y.; Zhan, X.; Yang, Q.; et al. Finite-time Consensus of Heterogeneous Multi-agent Systems by Integral Sliding Mode Control. *Int. J. Control. Autom. Syst.* **2024**, *22*, 1819–1826.
17. Ran, G.; Liu, J.; Li, C.; et al. Event-Based Finite-Time Consensus Control of Second-Order Delayed Multi-Agent Systems. *IEEE Trans. Circuits Syst. II Express Briefs* **2020**, *68*, 276–280.
18. Du, H.; Wen, G.; Wu, D.; et al. Distributed Fixed-Time Consensus for Nonlinear Heterogeneous Multi-Agent Systems. *Automatica* **2020**, *113*, 108797.
19. Zhang, J.; Lyu, M.; Shen, T.; et al. Sliding Mode Control for a Class of Nonlinear Multi-Agent System with Time Delay and Uncertainties. *IEEE Trans. Ind. Electron.* **2017**, *65*, 865–875.
20. Wu, Y.; Wang, Y.; Gunasekaran, N.; et al. Almost Sure Consensus of Multi-Agent Systems: An Intermittent Noise. *IEEE Trans. Circuits Syst. Express Briefs* **2022**, *69*, 2897–2901.
21. Xu, Y.; Li, K.; Dong, G.; et al. Resilient Cooperative Optimal Output Regulation Control for Nonlinear Multiagent Systems. *IEEE Trans. Cybern.* **2026**, *earyly access*.
22. Cai, J.; Feng, J.; Wang, J.; et al. Tracking Consensus of Multi-Agent Systems Under Switching Topologies via Novel SMC: An Event-Triggered Approach. *IEEE Trans. Netw. Sci. Eng.* **2022**, *9*, 2150–2163.
23. Ji, L.; Wang, C.; Zhang, C.; et al. Optimal Consensus Model-Free Control for Multi-Agent Systems Subject to Input Delays and Switching Topologies. *Inf. Sci.* **2022**, *589*, 497–515.
24. Ning, B.; Han Qing, L.; Ding, L. Distributed Finite-Time Secondary Frequency and Voltage Control for Islanded Microgrids with Communication Delays and Switching Topologies. *IEEE Trans. Cybern.* **2020**, *51*, 3988–3999.
25. Wang, Q.; He, W.; Zino, L.; et al. Bipartite Consensus for a Class of Nonlinear Multi-Agent Systems under Switching Topologies: A Disturbance Observer-Based Approach. *Neurocomputing* **2022**, *488*, 130–143.
26. Mu, X.; Hu, Z. Stability Analysis for Semi-Markovian Switched Stochastic Systems with Asynchronously Impulsive Jumps. *Sci. China Inf. Sci.* **2021**, *64*, 112206.
27. Long, T.; Yang, S.; Wang, Q.; et al. Finite-Time Consensus of Nonlinear Multi-Agent Systems via Impulsive Time Window

Theory: A Two-Stage Control Strategy. *Nonlinear Dyn.* **2021**, *105*, 3285–3297.

28. Feng, X.; Long, W. Reaching Agreement in Finite Time via Continuous Local State Feedback. In Proceedings of the Chinese Control Conference, 26–31 July 2007; pp. 711–715.
29. Li, X.; Peng, D.; Cao, J. Lyapunov Stability for Impulsive Systems via Event-Triggered Impulsive Control. *IEEE Trans. Automat. Contr.* **2020**, *65*, 4908–4913.